

Charge ordering in $\text{Bi}_{1-x}\text{Ca}_x\text{MnO}_3$ ($x \geq 0.75$) studied by electron-energy-loss spectroscopy

Y. Murakami and D. Shindo

Institute for Advanced Materials Processing, Tohoku University, Katahira, Sendai 980-8577, Japan

H. Chiba,* M. Kikuchi, and Y. Syono

Institute for Materials Research, Tohoku University, Katahira, Sendai 980-8577, Japan

(Received 14 August 1998; revised manuscript received 2 November 1998)

The effect of charge ordering of Mn^{3+} and Mn^{4+} ions on bonding features between oxygen $2p$ and manganese $3d$ orbitals in $\text{Bi}_{1-x}\text{Ca}_x\text{MnO}_3$ ($x \geq 0.75$) was studied along with the oxygen K edge by electron-energy-loss spectroscopy. A peak at 529 eV in the oxygen K edge was found to be sensitive to the manganese e_g hole content via strong hybridization between oxygen $2p$ and manganese $3d$ orbitals. It was demonstrated that the intensity was slightly reduced with the charge ordering in $\text{Bi}_{0.2}\text{Ca}_{0.8}\text{MnO}_3$. This effect was rationalized by considering such a mechanism that the strong hybridization with manganese $3d$ orbital was weakened as a result of the lattice distortion caused by the charge ordering, which was detected by a precise electron-diffraction method with energy-filtering and imaging plates. [S0163-1829(99)05509-5]

I. INTRODUCTION

Manganese oxides with the perovskite-type structure $R_{1-x}A_x\text{MnO}_3$ have attracted considerable attention because of the peculiar magnetism,¹ metal-to-insulator transformations² and charge ordering of Mn^{3+} and Mn^{4+} ions,³ etc., where R and A represent trivalent rare-earth and divalent alkaline-earth ions, respectively. Some of the phenomena seem to be rationalized by considering the behavior of e_g electrons in the manganese $3d$ orbital. For example, if the e_g electrons show an itinerant character, where the transfer interaction is large, ferromagnetism due to the double-exchange interaction appears. However, in several manganese oxides, the transfer interaction is reduced with cooling, and competing instabilities such as the charge-ordering interaction and antiferromagnetic superexchange, etc., become significant. Since the e_g electrons are mobile via migration of holes in the manganese $3d$ orbital (e_g holes), the above phenomena can be also discussed based on the nature of e_g holes. The content of e_g holes can be controlled by varying the relative content of A ions x . For example, the concentration of e_g holes tends to be enhanced with increasing x , while that of e_g electrons tend to be reduced.⁴ This is practically observed as a change in the relative concentration of Mn^{4+} ions to Mn^{3+} ones.

Recently, the effects of doping e_g electrons into an antiferromagnetic insulator CaMnO_3 , where e_g electrons are basically absent as far as the doping is not carried out, were studied along with partial substitution of Bi for Ca ($\text{Bi}_{1-x}\text{Ca}_x\text{MnO}_3$, $0.75 \leq x \leq 0.95$).^{5,6} It was found that the magnetic moment increased with the substitution ($x \geq 0.875$), exhibiting the maximum value of $1.1\mu_B$ at the Ca content $x = 0.875$. The conductivity was also enhanced with doping e_g electrons, although a completed metallic state was not achieved. These phenomena were explained to be attributed to the double-exchange interaction, which was realized by the doping of e_g electrons into the antiferromagnetic insulator. In the composition range $0.75 \leq x < 0.875$, however,

the competing instability of charge ordering became significant, and the ferromagnetism due to the double-exchange interaction was depressed. Actually, in $\text{Bi}_{0.2}\text{Ca}_{0.8}\text{MnO}_3$, superlattice reflections attributed to the charge ordering were observed by electron microscopy⁷ below 160 K, and the resistivity was largely enhanced below this temperature.

The conductive e_g electrons (or e_g holes) in perovskite manganese oxides migrate via the oxygen $2p$ orbital, which is strongly hybridized with the manganese $3d$ orbital. Because of this fact, the conductivity of e_g electrons (or e_g holes) is largely affected by a feature of Mn-O-Mn bonding, i.e., deviation of the bond angle from 180° . For example, in $\text{La}_{1-x}\text{Sr}_x\text{MnO}_3$ ($x = 0.17$), the conductivity in a rhombohedral phase was shown to be larger than that in an orthorhombic phase, where the angular distortion in the former was smaller than that in the latter.⁸ This is because the transfer interaction is reduced with increasing the angular distortion through changes in electronic bandwidth, etc. It has been demonstrated that the transfer interaction was also affected by varying the averaged ionic radius of the ($R_{1-x}A_x$) site in the perovskite structure,⁸⁻¹⁰ i.e., it is also responsible for the bandwidth, while this effect seems to be rather small in the present system because of the similar ionic radii between Bi and Ca. It is expected that the observed changes in electric and magnetic properties associated with the charge ordering in $\text{Bi}_{0.2}\text{Ca}_{0.8}\text{MnO}_3$ (Refs. 5, 7) are also accompanied by some state change in the Mn-O-Mn bonding, while a detailed investigation has not been carried out for this problem.

The purpose of the present work is to investigate the effect of charge ordering on bonding features between oxygen $2p$ and manganese $3d$ orbitals in $\text{Bi}_{1-x}\text{Ca}_x\text{MnO}_3$ by electron-energy-loss spectroscopy (EELS) coupled with a precise electron-diffraction method with energy filtering.

II. EXPERIMENTAL PROCEDURE

A way to fabricate $\text{Bi}_{1-x}\text{Ca}_x\text{MnO}_3$ ($0.75 \leq x \leq 0.95$) ceramic specimens was described in the previous paper in

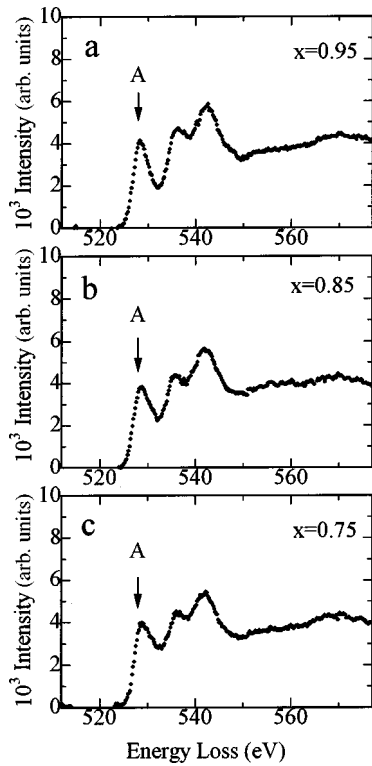


FIG. 1. Electron-energy-loss spectra of the oxygen K edge acquired from $\text{Bi}_{1-x}\text{Ca}_x\text{MnO}_3$ ($x=0.95, 0.85,$ and 0.75) at room temperature. The peak at 529 eV is defined as “peak A” in the text.

detail.^{5,6} Oxygen content of the fabricated specimens was in the range 2.98–3.01,⁶ which were determined by an iodine titration method. It was ascertained by both electron microscopic observations and powder x-ray-diffraction measurements that the crystal structure of $\text{Bi}_{1-x}\text{Ca}_x\text{MnO}_3$ was pseudocubic ($Pbmm$) at room temperature in the composition range $0.75 \leq x \leq 0.95$.⁶ Electron-energy-loss spectra were measured at 293 K for the room-temperature phase ($x=0.75, 0.80, 0.85$ and 0.95), and at 130 K for the low-temperature phase (in a charge-ordered state, $x=0.80$) by utilizing a Gatan PEELS System 666 attached to a transmission electron microscope (JEM-2010). Those spectra were measured in the image mode at magnification of $\times 10,000$ with an objective aperture of 10 mrad, where every specimen was in nonaxial conditions. A spectrometer collection aperture of 1 mm was employed, and the dispersion setting was 0.2 eV/channel. The energy resolution was between 1.8 and 2.0 eV. Electron-diffraction patterns were recorded in a quantitative manner by using imaging plates^{11,12} (Fuji FDL-UR-V). To precisely observe the intensity distribution of the superlattice reflections, the strong background in electron-diffraction pattern was reduced by utilizing a recently developed omega-type energy filter which was attached to a JEM-2010 electron microscope.

III. RESULTS AND DISCUSSION

Figure 1(a) shows a typical electron-energy-loss spectrum of the oxygen K edge acquired from $\text{Bi}_{1-x}\text{Ca}_x\text{MnO}_3$ ($x=0.95$) at room temperature, where the background component was subtracted by means of a curve-fitting method.¹³ Here, the energy-loss value was calibrated by setting the

manganese L_3 edge at 641.0 eV, which was visible in a higher energy-loss region. In electron-energy-loss spectroscopy, a prominent peak is visible at the threshold (i.e., near the Fermi level) of the K edge if some amount of $2p$ density-of-states are vacant, since the K edge is attributed to electronic excitations from $1s$ to $2p$ bands. (Strictly speaking, excitations satisfying the dipole selection rule $\Delta l = \pm 1$ are permitted.) Hence, the fine structure in Fig. 1(a) represents that the oxygen $2p$ orbital is partially vacant in this oxide. As mentioned in the previous section, hole content of perovskite manganese oxides can be controlled by substitution of trivalent alkaline-earth ions for divalent rare-earth ones, where the substitution is thought to directly affect the valency of manganese $3d$ orbital rather than that of oxygen $2p$ one. This point is reasonable if we consider that manganese ions can take a few different ionic states,⁴ such as Mn^{3+} and Mn^{4+} , while in oxygen the O^{2-} state is the most stable where the $2p$ orbital is entirely occupied. The presence of a peak at the threshold of oxygen K edge in this specimen can be elucidated as in the following. Since the oxygen $2p$ orbital is extended to the same direction as that of the manganese $3d$ (e_g) orbital in this oxide, they are strongly hybridized to each other. Thus, some amount of holes in the manganese $3d$ orbital are thought to be occupied by the oxygen $2p$ orbital as a result of the strong hybridization. This feature was also pointed out in some other types of manganese oxides such as Mn_2O_3 , etc.^{14,15} In manganese oxides, the manganese $3d$ levels are splitting due to the crystal field, and the magnitude of splitting is dependent on materials. For example, a relatively large splitting (e.g., 3.3 eV) was observed in MnO_2 ,¹⁵ while that of the perovskite-type oxides is believed to be smaller (e.g., 1–2 eV). This point was actually confirmed in some recent investigations.¹⁶ The energy resolution in the present EELS measurements is 1.8–2.0 eV, which was determined by the full width at half maximum of the zero-loss peak. But the actual resolution in a higher energy-loss region, e.g., around the oxygen K edge, may be somewhat poorer than this value due to the character of the utilized spectrometer. Hence, it is thought that the small splitting of the manganese $3d$ levels is not clearly seen in the oxygen K edge with the present energy resolution.

Then, we expect that a peak near the Fermi level in the oxygen K edge will show a meaningful change with the manganese e_g hole content if it is directly related with the hybridization between manganese $3d$ and oxygen $2p$ orbitals. To check this point, energy-loss spectra were acquired from the oxides with different Ca content, i.e., where the e_g hole content tends to be enhanced with increasing Ca content. The results were shown in Figs. 1(b) ($x=0.85$) and (c) ($x=0.75$). It was ascertained that similar fine structures to that of $x=0.95$ were observable in the both cases. Changes in the peak positions were not observed within the experimental accuracy. However, we notice a systematic change in the peak profile at 529 eV, which is just above the Fermi level, while an appreciable change was not observed in the other ones at 536 and 542 eV. The peak at 529 eV is hereafter called peak A. To inspect this composition dependence more in detail, intensity of the peak A was plotted as a function of Ca content in Fig. 2. Here, integrated intensity of the peak A was determined by means of a profile fitting method with Gaussian functions as shown in the inset in Fig. 2. It was

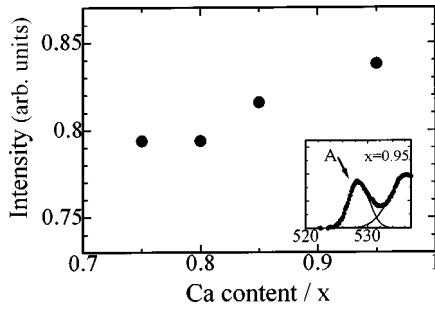


FIG. 2. Composition dependence of intensity of the peak at 529 eV. See text for details.

then normalized with the peak intensity of the one at 536 eV, which did not show an appreciable change in this composition range, for the sake of a quantitative comparison. It was found that the intensity of peak A tended to be enhanced with increasing Ca content. In Fig. 2, the result of $x=0.80$ was obtained from thin-foiled specimens prepared by ion milling, which were originally prepared for detailed observations of the structural transformation upon cooling, while the other ones were from powder specimens (crushed specimens), i.e., for example, the surface condition of the thin-foiled specimens may be somewhat different from the crushed specimens. Hence, the difference of the specimen preparations may cause some numerical deviation of the data between $x=0.80$ and the other ones. If we observe the peak profile in Fig. 1 carefully, the profile change in the peak A seems to occur at the high-energy side of this peak, i.e., some broadening of the peak may take place at the high-energy side. Zampieri *et al.*¹⁷ recently carried out a careful x-ray-absorption spectroscopy (XAS) measurement of the oxygen $1s$ spectra of CaMnO_3 with an energy resolution of 0.6 eV. They discovered a small splitting of the peak at the threshold, and this was interpreted as the splitting of the manganese $3d$ levels. If we consider this point, the small broadening in the peak A in Fig. 1 may be due to the change in the crystal-field splitting of the manganese $3d$ levels with composition. However, this slight peak broadening does not disturb the present investigation, since we are interested in the composition dependence of the total intensity of peak A, which is related to the unoccupied density of states. The result of Fig. 2 explicitly indicates that the manganese e_g hole content is reflected on the intensity of peak A of the oxygen K edge via the strong hybridization. Thus, we can conclude that the peak at 529 eV in the oxygen K edge is closely related to the hybridization between the oxygen $2p$ and manganese $3d$ orbitals.

If we try to perfectly describe the intensity of the peak A, we may have to also consider the hybridization between oxygen $2p$ and manganese t_{2g} levels in addition to the one between oxygen $2p$ and manganese e_g levels. However, in the interpretation of the result of Fig. 2, the latter one seems to play an important role rather than the former one. In the electron-doped (or hole doped) perovskite manganese oxide, the manganese $t_{2g\uparrow}$ band is basically fully occupied while the $e_{g\uparrow}$ band, where the Fermi level is located, is only partially occupied. The presence of unoccupied $e_{g\uparrow}$ states just above the Fermi level was actually shown in a recent investigation for CaMnO_3 .¹⁷ Thus, electron doping (or hole doping) will dominantly change the occupancy of the $e_{g\uparrow}$ band, and this is

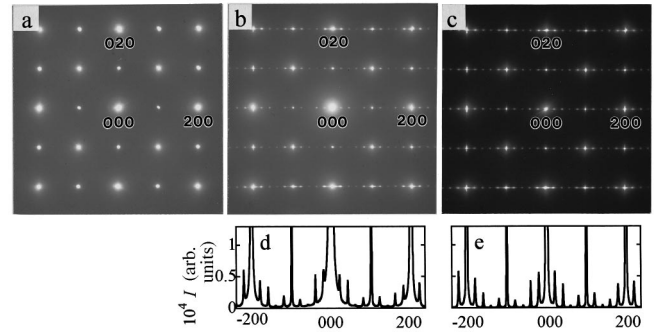


FIG. 3. Conventional electron-diffraction patterns of $\text{Bi}_{0.2}\text{Ca}_{0.8}\text{MnO}_3$ (a) at 293 K and (b) at 130 K (in a charge-ordered state). (c) Electron-diffraction pattern after reducing the background in (b) by energy filtering. Intensity profiles of superlattice reflections visible in (b) and (c) were represented in (d) and (e), respectively. Both the room-temperature and low-temperature phases were indexed by using a unit cell of $a \sim \sqrt{2}a_p$, $b \sim \sqrt{2}a_p$, and $c \sim 2a_p$ (Refs. 6 and 7), where a_p represents the lattice constant of the simple perovskite structure.

thought to be well reflected on the peak intensity at the threshold of the oxygen K edge. The systematic change in the peak intensity at the threshold with hole doping was also observed in $\text{La}_{1-x}\text{Ca}_x\text{MnO}_3$ by means of XAS measurements.¹⁸ As far as these points are considered, we believe that the change in the peak intensity observed in Fig. 2 is mainly due to the change in the hole content of the $e_{g\uparrow}$ levels.

It was recently reported that $\text{Bi}_{1-x}\text{Ca}_x\text{MnO}_3$ ($0.75 \leq x < 0.875$) exhibited charge ordering of manganese ions with cooling.^{5,7} Figure 3(a) shows a conventional electron diffraction pattern at room temperature, while Fig. 3(b) was taken in a charge-ordered state at 130 K. The charge ordering is observable as the appearance of superlattice reflections along the a^* axis (or the b^* axis) of the room-temperature phase as shown in Fig. 3(b). To discuss structural changes with charge ordering, those diffraction patterns should be analyzed so carefully. However, since the superlattice reflections are quite weak, the precise observations are sometimes disturbed by the strong background in electron-diffraction patterns, which originates from inelastic scattering such as plasmon scattering. To reduce the strong background, in the present work, inelastically scattered electrons were removed by using a recently developed omega-type energy filter.¹⁹ In this method, transmitted electrons are energy dispersed by the omega-type magnet, and we can obtain an electron-energy-loss spectrum. Then, if an energy slit is inserted in the spectrum so as to select elastically scattered electrons alone, contributions of inelastic scattering can be eliminated. Figure 3(c) shows an electron-diffraction pattern after the energy filtering, which was taken from the same region at the same temperature as those in Fig. 3(b). We notice that the strong background has been effectively removed, and the weak superlattice reflections can be observed much clearly. The efficiency of the background subtraction is apparent if we compare the intensity profiles in Figs. 3(d) and 3(e) to each other. (It is noted that peak positions of superlattice reflections were dependent on observed specimens and regions, although the characteristic feature in the intensity profile as described below was observed in every case. The na-

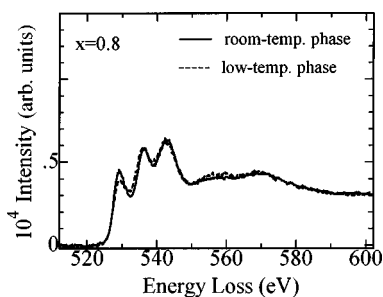


FIG. 4. Changes in the oxygen K edge associated with charge ordering in $\text{Bi}_{0.2}\text{Ca}_{0.8}\text{MnO}_3$. See text for details.

ture of the appearance of the superstructures with different periodicity will be discussed elsewhere.)

By virtue of the precise electron-diffraction method with energy filtering and imaging plates, some crystallographic features of the charge ordering in $\text{Bi}_{0.2}\text{Ca}_{0.8}\text{MnO}_3$ were disclosed, and they can be summarized as in the following. First, it was confirmed that the charge ordering was accompanied by an appreciable lattice strain, which is thought to originate from the Jahn-Teller effect of Mn^{3+} ions. Presence of the periodic lattice strain in the charge-ordered state is evidenced by the feature of the intensity distribution of the superlattice reflections [Fig. 3(e)], where the intensity is asymmetric around the fundamental reflections, i.e., higher intensity at larger scattering angle.^{7,20,21} Although the difference of the scattering amplitudes between Mn^{3+} and Mn^{4+} is too small to create obvious superlattice reflections as shown in Fig. 3(e), they can be detected as the periodic lattice strain attributed to the charge ordering. Secondly, the orthorhombic distortion, which was evaluated at a/b , was found to be slightly enhanced with the charge ordering, where a and b represent the lattice parameter along $[100]$ and $[010]$ axes, respectively. In the room-temperature phase, the oxide showed pseudocubic symmetry ($a/b \approx 1.00$). However, in the low-temperature phase, the orthorhombic distortion was about 0.99, which represents a change in the symmetry from pseudocubic to orthorhombic with charge ordering. This orthorhombicity is thought to originate from a distortion of the Mn-O-Mn bond angle, as in the case of other perovskite manganese oxides such as $\text{La}_{1-x}\text{Sr}_x\text{MnO}_3$,⁸ and this effect is to be related with the periodic lattice strain creating the superlattice reflections.

Considering the crystallographic changes with charge ordering as described above, electron-energy-loss spectra of the oxygen K edge were measured from both the room-temperature phase (293 K) and the low-temperature phase (130 K, in a charge-ordered state) in $\text{Bi}_{0.2}\text{Ca}_{0.8}\text{MnO}_3$. The results were shown in Fig. 4, in which both the spectra were acquired from the same position in a specimen to eliminate a spectrum modulation effect due to difference in specimen thickness. It was found that the intensity of peak A of the low-temperature phase (dashed-line) was slightly weaker than that of the room-temperature phase (solid-line). Magnitude of the intensity change was basically small and dependent on observed regions. Furthermore, the spectra were sometimes modulated by the radiation damage, when the incident electron beam was strong. These points disturbed the quantitative analysis for this problem. However, the above tendency was derived from the repeated measurements with

several specimens. It may be seen that there is a quite small change in the peak profile at around 536 eV, where the peak seems to be somewhat broadened with the phase transformation. However, the intensity change of peak A is much larger than that of the peak at around 536 eV upon cooling, e.g., the former is reduced about 20% with the transformation while the latter is increased only 2% as far as the result in Fig. 4 is analyzed. The magnitude of the intensity change should be carefully discussed along with the spectra collected with a higher-energy resolution elsewhere. Despite this fact, we can say in the present investigation that the principal feature of the change in the oxygen K edge with charge ordering is the reduction of the peak intensity at 529 eV.

As described in the previous section, the peak at 529 eV is thought to be closely related with the hybridization between oxygen $2p$ and manganese $3d$ orbitals, and the intensity was shown to be sensitive to the manganese e_g hole content. In the case of Fig. 4, however, the total hole content is equal between the two spectra, since they were acquired from the same position of the same specimen. Thus, the observed effect is to be due to some state change in the hybridization. It is interpreted for the experimental result that the strong hybridization between oxygen $2p$ and manganese $3d$ orbitals are somewhat weakened as a result of the charge ordering. This interpretation can be supported by the following aspects of the structural transformation. As mentioned in the previous part, the orthorhombic distortion is somewhat enhanced with the charge ordering. This is thought to be caused by the distortion of Mn-O-Mn bond angle, i.e., enhancement of deviation from 180° . Since the distortion reduces the transfer of e_g holes (e_g electrons),⁸ it will contribute to weaken the strong hybridization between oxygen $2p$ and manganese $3d$ orbitals. Actually, in the present system of $\text{Bi}_{0.2}\text{Ca}_{0.8}\text{MnO}_3$, a significant increase of the electric resistance was observed below the charge-ordering temperature at 160 K.^{5,7} Hence, it was demonstrated that the peak at 529 eV was sensitive not only to the e_g hole content but also to the state of hybridization between oxygen $2p$ and manganese $3d$ orbitals, and the latter was shown to be affected by the charge ordering. Similar fine structures in the oxygen K edge were also observed in $\text{La}_{1-x}\text{Sr}_x\text{MnO}_3$ ($0 \leq x \leq 0.7$),²² where a peak at the threshold was shown to be related with the conductivity, although changes in the fine structures with charge ordering were not discussed.

The reduced intensity of the peak A with charge ordering was rationalized by considering the weakened hybridization between oxygen $2p$ and manganese $3d$ orbitals. This will be reasonable if we consider that enhancement of the orthorhombic distortion, which depresses the transfer of e_g holes (e_g electrons), occurs with the structural transformation. However, to perfectly explain the intensity change of the peak A with charge ordering, we should also take into consideration the difference of energy levels between the oxygen $2p$ and manganese $3d$ orbitals, which may be somewhat changed with the structural transformation. This point, which may be also responsible for the weakened hybridization, should be investigated by measurements with a higher energy resolution in the future.

To summarize, a change in the oxygen K edge with charge ordering was observed by electron-energy-loss spectroscopy in $\text{Bi}_{0.2}\text{Ca}_{0.8}\text{MnO}_3$, where intensity of the peak at

529 eV was reduced with the charge ordering. This peak was shown to be closely related with the hybridization between oxygen $2p$ and manganese $3d$ orbitals by analyzing the composition dependence of peak intensity. The observed intensity change in $\text{Bi}_{0.2}\text{Ca}_{0.8}\text{MnO}_3$ was rationalized by considering such a mechanism that the strong hybridization was somewhat weakened as a result of the distortion of Mn-O-Mn bond angle, which was caused by the charge ordering. In general, the most favorable condition for the occurrence of charge ordering is that the concentrations of Mn^{3+} and Mn^{4+} are equivalent. However, it was ascertained in the present work that an appreciable change in the electronic structure (hybridization) was observed even in the present e_g electron-

doped system of $\text{Bi}_{0.2}\text{Ca}_{0.8}\text{MnO}_3$, where the concentration of Mn^{3+} was much smaller than that of Mn^{4+} . This effect seems to be an essential feature of charge ordering in perovskite manganese oxides.

ACKNOWLEDGMENTS

The authors are grateful to T. Kaneyama and Dr. T. Oikawa at JEOL Ltd. for their help in utilizing the omega-type energy filter. This work was supported by a Grant-in-Aid for Scientific Research on Priority Area and for the Encouragement of Young Scientists (Y. M.) from the Ministry of Education, Science and Culture of Japan.

*Present address: Magnetic Disk Drive Group, Second Manufacturing Dept., Yamagata Fujitsu Ltd., Higashine 999-3701, Japan.

¹For example, Y. Tokura *et al.*, Phys. Rev. Lett. **76**, 3184 (1996).

²For example, H. Kuwahara *et al.*, Science **270**, 961 (1995).

³For example, C. H. Chen and S.-W. Cheong, Phys. Rev. Lett. **76**, 3188 (1996).

⁴E. O. Wollan and W. C. Koehler, Phys. Rev. **100**, 545 (1955).

⁵H. Chiba *et al.*, Solid State Commun. **99**, 499 (1996).

⁶H. Chiba *et al.*, Solid State Ionics **108**, 193 (1998).

⁷Y. Murakami *et al.*, Phys. Rev. B **55**, 15 043 (1997).

⁸A. Asamitsu *et al.*, Nature (London) **373**, 407 (1995).

⁹J. B. Torrance *et al.*, Phys. Rev. B **45**, 8209 (1992).

¹⁰A. Sundaresan *et al.*, Phys. Rev. B **57**, 2690 (1998).

¹¹D. Shindo *et al.*, Ultramicroscopy **54**, 221 (1994).

¹²A. Taniyama, D. Shindo, and T. Oikawa, J. Electron Microsc.

16, 303 (1997).

¹³R. F. Egerton, *Electron Energy-Loss Spectroscopy in the Electron Microscope* (Plenum, New York, 1986).

¹⁴H. Kurata *et al.*, Phys. Rev. B **47**, 13 763 (1993).

¹⁵H. Kurata and C. Colliex, Phys. Rev. B **48**, 2102 (1993).

¹⁶For example, S. Satpathy, Z. S. Popovic, and F. R. Vukajlovic, Phys. Rev. Lett. **76**, 960 (1996).

¹⁷G. Zampieri *et al.*, Phys. Rev. B **58**, 3755 (1998).

¹⁸J. H. Park *et al.*, Phys. Rev. Lett. **76**, 4215 (1996).

¹⁹D. Shindo *et al.*, Jpn. J. Appl. Phys., Part 1 **37**, 2593 (1998).

²⁰J. M. Cowley, *Diffraction Physics* (North-Holland, Amsterdam, 1975).

²¹B. J. Sternlieb *et al.*, Phys. Rev. Lett. **76**, 2169 (1996).

²²H. L. Ju, H.-C. Sohn, and K. M. Krishnan, Phys. Rev. Lett. **79**, 3230 (1997).